Published online 18 September 2006 *Nucleic Acids Research, 2006, Vol. 34, No. 17* ***4893–4899***
doi:10.1093/nar/gkl434

Identification of a structural and functional domain in xNAP1 involved in protein–protein interactions

Christine Friedeberg, Garry Scarlett, John McGeehan, Anita Abu-daya, Matthew Guille and Geoff Kneale*

Institute of Biomedical and Biomolecular Sciences, University of Portsmouth, Portsmouth PO1 2DT, UK

Received March 13, 2006; Revised May 18, 2006; Accepted June 1, 2006

ABSTRACT

xNAP1 (*Xenopus* nucleosome assembly protein) belongs to the family of nucleosome assembly proteins (NAPs) and shares 92% identity with human and mouse NAP1. NAPs have been reported to have a role in nucleosome assembly, cell cycle regulation, cell proliferation and transcriptional control, although the precise function of NAP1 is still not clear. Here we report the identification of a putative domain of xNAP1 by limited proteolysis. This domain has been mapped in the xNAP1 protein sequence to residues 38–282 and thus lacks the acidic sequences at the N- and C-termini. We have studied this domain and related fragments *in vitro* and by a functional assay involving over-expression of the protein in *Xenopus laevis* embryos. Analytical ultracentrifugation shows that removal of the acidic N- and C-terminal regions does not prevent the formation of larger multimers, which are predominantly hexadecamers. Injection of mRNA encoding the full-length xNAP1 or the putative domain and other related constructs into *Xenopus* embryos gave identical phenotypes. These results are discussed in relation to protein–protein interactions between NAP1 octamers and a possible 'squelching' mechanism.

INTRODUCTION

Xenopus nucleosome assembly protein (xNAP1) is a protein of 392 residues and a molecular mass of 45 258 Da, although it migrates anomalously as ~60 kDa species as assayed by SDS–PAGE. xNAP1 is a member of a family of proteins that share the ability to assemble histones into nucleosomes on DNA *in vitro*. NAP1 proteins are universally present in eukaryotic cells (1) and have homology with nucleosome assembly proteins (NAPs), nucleoplasmin and N1/N2 in the acidic C-terminus region (1). All these proteins possess negatively charged regions, which have been suggested to promote nucleosome assembly *in vitro* (2,3). xNAP1 is closely related to human and mouse NAP1, sharing 92% identity with these proteins.

Experiments on *Drosophila* NAP1 (4) revealed that dNAP1 associates with H2A and H2B and that the protein is found in the nucleus during S phase but is mainly cytoplasmic during G_2 phase. NAP1 acts as a core histone shuttle, delivering histones from the cytoplasm to the nucleus where chromatin assembly takes place. Recent studies have indicated a novel role for yNAP1 as a mediator of chromatin fluidity, by incorporating histone variants into chromatin and assisting nucleosome sliding (5). In this model, NAP1 has a much more active role in shaping chromatin structure. Histone variants locally alter chromatin structure, with histone chaperones and other cellular factors promoting histone exchange and chromatin fluidity (6). It is believed that these processes can facilitate the interchange between different chromatin states, having varying degrees of transcriptional activity (6).

Other studies have also linked NAPs with gene regulation. NAP1 and NAP2 have been reported to form a complex with p300 (7). Histone acetylation by p300 promotes the transfer of H2A and H2B to NAP1 *in vitro* (8) potentially leading to transcriptional activation mediated by disruption of the histone octamer. In another study, xNAP1 was shown to have a transcriptional role in embryonic blood formation. xNAP1 is expressed tissue specifically in the ectoderm, precisely overlying the ventral blood island and the outer globin expressing cells (9). Depletion of xNAP1 in embryos showed that mRNA levels of haematopoietic marker genes SCL and AML decreased significantly but endothelial markers Hex and Fli-1 were unaffected. Since depletion of xNAP1 led to gene-specific changes, it was proposed that xNAP1 has a role in tissue restricted gene regulation (10).

There are a variety of conserved regions in NAP1 sequences. There are three negatively charged regions, including a large acidic region at the C-terminal and a smaller

*To whom correspondence should be addressed. Tel: 0044 2392 842678; Fax: 0044 2392 842053; Email: Geoff.Kneale@port.ac.uk
Present addresses:
John McGeehan, EMBL-Grenoble, Grenoble Cedex 9, France
Anita Abu-daya, NIMR, The Ridgeway, Mill Hill, London NW7 1AA, UK

one at the N-terminal. Studies on yNAP1 have revealed that the acidic C-terminal region is dispensable for nucleosome assembly *in vitro* (11), but that it is required for the dissociation of H2A/H2B dimers from nuclear core particles, whereby yNAP1 can subsequently facilitate nucleosome sliding along the DNA to a thermodynamically favourable position (5). dNAP1 has two PEST regions and a possible PEST region has also been identified in xNAP1 (9). Nuclear localization (NLS) and nuclear export signals (NES) also appear to be conserved in NAPs (4,9,12,13). Studies by Li *et al*. (12) identified a phosphorylation site adjacent to the NLS sequence in dNAP1, and it has been suggested that this plays a role in the translocation of NAP1 between the cytoplasm and nucleus.

The yNAP1 NES sequence is necessary for shuttling the protein from the nucleus to the cytoplasm. Failure to do so was found to inhibit mitotic progression (13). The NES sequences have been shown to align in yeast, nematode, *Xenopus*, *Drosophila* and human NAP1 (13). A KGIPEFWLT and a SFFNFF sequence are also conserved in NAP1s across these species (1,4,11). Although the KGIPEFWLT region has been assigned no structural or functional role, the SFFNFF sequence is necessary for nucleosome assembly (11).

Secondary structure analysis of the yeast orthologue, yNAP1, by circular dichroism spectroscopy (14) indicates that the C-terminal domain (approximately one-third of the protein) is mostly unstructured with ~25% α-helix content. Removal of residues 354–365 (PRAVDWFTGAALE) located adjacent to the C-terminal acidic region caused a substantial loss of α-helical structure. Recent studies (15,16) suggest that NAP1 forms dimers, octamers and hexadecamers in a concentration-dependent manner. Both the dimer and the octamer of NAP1 appear to bind histones H2A and H2B in a one NAP1 monomer per histone monomer ratio, but the hexadecamer appears not to be involved in histone interactions. Based on this, a model for cell cycle-dependent shift of the NAP1 dimer–octamer equilibrium has been proposed that reflects different biological functions of NAP1 (16). According to this model, the low concentrations of NAP1 in the nucleus at G_1 lead to dimer formation and a role in gene regulation via chromatin rearrangement. Accumulation of NAP1 in the nucleus during S phase leads to formation of octamers capable of carrying multiple H2A.H2B dimers to replication sites.

In this article we define a structural domain of xNAP1 by limited proteolysis. We show that this domain multimerizes, forming predominantly hexadecameric complexes *in vitro,* and that over-expression of the domain affects axial patterning in *Xenopus*, despite the lack of several of the conserved regions believed to be important for activity.

MATERIALS AND METHODS

Cloning of expression constructs

Full-length and deletion constructs of xNAP1 were amplified by PCR using Vent DNA polymerase (NEB) before cloning. These NAP1 sequences were ligated into NcoI/XhoI restricted pET28b(+) (Novagen) and XbaI/XhoI restricted pBUT plasmids. Recombinants in each case were fully sequenced to confirm the presence of the insert.

Protein expression and purification

Expression of NAP1 and truncations thereof was carried out in 500 ml 2xYT broth with 50 μg ml^{-1} kanamycin antibiotic inoculated with 10 ml of an overnight culture of *Escherichia coli* BL21(DE3) pLysS. The culture was incubated at 37°C by shaking until mid-log phase. Protein expression was induced by 1 mM IPTG, and the cells incubated for a further 3 h before harvesting. The sample was lysed by sonication (Vibracell™ VCX 500 Jencons-PLS) and the soluble fraction isolated by centrifugation. Recombinant protein was purified using a Hi-trap chelating column (Amersham Pharmacia) followed by preparative size exclusion chromatography on a superose 12 column.

Limited proteolysis of xNAP1

NAP1 was subjected to limited proteolysis with either chymotrypsin or trypsin (Sigma). The enzymes were dissolved in 1 mM HCl to make 5 mg ml^{-1} stock solutions, and aliquots were frozen at −20°C. The enzymes were added to the xNAP1 (0.4 mg ml^{-1}) sample at an enzyme to substrate (w/w) ratio of 1:10 000 in a buffer of 100 mM sodium phosphate at pH 7.0, 100 mM NaCl, 1 mM EDTA and 1 mM DTT. The reactions were incubated at 25°C. Aliquots were taken at various time points and the reaction was stopped by the addition of PMSF (1 mM final concentration). Samples were analysed on 10% SDS–PAGE gels, followed by staining with Coomassie blue.

Embryo manipulation

Embryos were obtained as described by Smith and Slack (17) and staged according to Nieuwkoop and Faber (18). *In vitro* transcription and microinjection of mRNA was carried out as described previously (19,20). Injections of mRNA were carried out at the 1-cell stage with 4 nl of RNA solution (37 pg RNA total).

Mass spectroscopy

The digested xNAP1 samples were sent for mass spectrometry to M-Scan Ltd, Wokingham. Salts were removed from the 1 ml sample by washing on a desalting column with 0.1% aqueous formic acid, and the retained analytes were eluted in a solvent of aqueous acetonitrile. The desalted sample was loaded into a nanospray needle (MDS Protana) and analysed using a Sciex Q-Star/Pulsar, 'Q-TOF' mass spectrometer (MDS Sciex) operating in positive electrospray mode. Data were collected by MCA acquisition and interpreted by manual inspection of the multiply charged species observed in the spectrum.

Dynamic light scattering

Dynamic light scattering (DLS) was performed on purified T2 protein at 20°C using a Protein Solutions DynaPro temperature-controlled microsampler. The samples were in gel filtration buffer containing 10% glycerol and centrifuged at 14 000 r.p.m. at 4°C for 10 min before DLS. From the resulting hydrodynamic radius, R_h, an upper estimate of the molecular mass, M_r, of the protein was obtained using the empirical relationship for typical globular proteins: $M_r = (1.68 \times R_h)^{2.34}$ using the supplied software.

Analytical ultracentrifugation

A Beckman Optima XL-A analytical ultracentrifuge (Beckman-Coulter, Palo Alto, CA, USA) was used for sedimentation equilibrium experiments. All measurements were recorded at 20°C. T2 protein was purified by metal chelate affinity chromatography and size exclusion chromatography on a Superdex 75 column, using the T2 buffer with an additional 10% glycerol. The protein was dialysed overnight into AUC buffer (100 mM triethanolamine, 50 mM KCl, 1 mM EDTA and 10% glycerol, pH 8.5). The experiment was performed in six-channel cells of 12 mm optical path length, using 90 μl of solution at three protein concentrations (0.14, 0.07 and 0.035 mg ml^{-1}). AUC buffer (100 μl) was loaded into the corresponding channel. The rotor was accelerated to 3000 r.p.m. and scans of absorbance versus radial displacement were taken at 280 nm every 5 h for over 24 h and again after a total of 48 h; equilibrium was seen to be reached after 20 h. Scans were analysed using the Beckman XL-A software. However, the lower concentration samples could not be fitted with any degree of accuracy and were not subsequently used.

RESULTS

xNAP1 contains structural domains resistant to proteolytic digestion

Limited proteolysis is a sensitive technique that can be used to examine the tertiary structure of proteins, since tightly folded domains are more resistant to proteolysis. We therefore chose this approach to identify structural domains within xNAP1. In separate experiments, xNAP1 was digested with the proteases trypsin or α-chymotrypsin. Samples were taken at various time intervals over a 2 h period. Trypsin digestion (Figure 1a) produces a prominent fragment that has an apparent molecular mass of ~50 kDa (T1). Digestion with α-chymotrypsin (Figure 1b) also reveals a prominent fragment (C1) of ~50 kDa; in both the cases the band corresponding to the intact protein decreases in intensity. Digestion with trypsin when extended over 24 h resulted in the appearance of a major 35 kDa (T2) fragment (Figure 1c). In contrast, after a 24 h digestion of xNAP1 with α-chymotrypsin the C1 fragment is still the predominant band, although two faint additional bands, ~35–37 kDa, in size are visible. These faint bands are labelled C2 (i) and (ii) (Figure 1c). After 24 h of digestion the samples were passed down a nickel Hi-trap column (Amersham), and both the T2 and C1 fragments were found in the flow through. Since the divalent ion chelating His-tag is at the N-terminus of the purified recombinant xNAP1, and neither fragment is capable of chelating nickel, the T2 and C1 fragments must lack the N-terminus.

Proteolytic fragments C1 and T2 map to overlapping regions of the xNAP1 sequence

We next determined the molecular mass of the xNAP1 putative structural domains T2 and C1 by mass spectroscopy. Samples were digested with the respective enzymes under limiting conditions and sent lyophilized for ESI mass spectrometry. The mass spectrometry results of the xNAP1 sample digested with α-chymotrypsin showed that the largest fragment observed is 39 500 Da in size, while mass spectroscopy of the trypsin digested sample detected three major fragments between 27 826 and 28 970 Da. Since xNAP1 runs anomalously on SDS–PAGE, we used 2D IEF to compare the pI of both the T2 and C1 proteolytic fragments with that of the full-length protein. T2 and C1 were found to have a pI of ~4.8 and ~5.2, respectively, comparable with the full-length xNAP1 pI of ~5.2, and therefore both T2 and C1 can be expected also to run anomalously.

The T2 and C1 proteolytic fragments were also analysed by N-terminal sequencing. The N-terminal sequence of C1 was identified as ALQERLDD and the N-terminal sequence of the T2 fragment was identified as QLTAQM. These N-termini are located only 13 amino acids apart in the xNAP1 sequence. The C-termini of the fragments C1 and T2 were predicted by determining the theoretical digestion sites of trypsin and α-chymotrypsin in the xNAP1 sequence in conjunction with the mass spectroscopy data. The C1 sequence was mapped onto a fragment of 342 amino acids with a predicted mass of 39 537 Da. The identification of the T2 N-terminal sequence, together with the known proteolytic sites within the xNAP1 protein sequence, give predicted molecular masses for three putative fragments: 27 850 (239 amino acids), 28 560 (245 amino acids) and 28 973 Da (249 amino acids). These masses are very similar to those of the three major peaks obtained by mass spectroscopy (27 826, 28 560 and 28 970 Da). The 28 560 Da fragment ends closest to the NLS sequence, but not within it, and was therefore chosen for further studies. The T2 and C1 structural domains are shown in Figure 2.

The T2 domain forms hexadecameric complexes *in vitro*

To facilitate analysis of the putative T2 domain the DNA sequence encoding the T2 fragment was subcloned into the pET-28b plasmid vector, allowing bacterial expression of the domain as a histidine tagged fusion. The recombinant T2 protein was expressed and purified before being assayed by analytical ultracentrifugation and dynamic light scattering (DLS). DLS shows the presence of any polydispersity in the sample and gives the hydrodynamic radius (R_h) of the components. A major component (>90%) was observed with a hydrodynamic radius of ~9 nm (Figure 3), indicating that the T2 domain forms discrete multimers. It is not possible to calculate a true molecular weight from the R_h except for spherical particles, as significant asymmetry and/or unstructured tails lead to an overestimate of the M_r. In addition, the histidine tag, being unstructured and extended, will lead to a further increase in R_h over and above that owing to asymmetry, and hence would further overestimate the molecular weight.

We therefore performed sedimentation equilibrium on the recombinant T2 domain in order to determine more precisely the size of the protein complexes. The concentration distribution at equilibrium depends only on molecular mass, and is independent of the shape of the molecule. Figure 4 shows the equilibrium distribution of the T2 sample at 0.14 mg ml^{-1}. When fitted to a single species model, the average molecular mass of the sample was 430 kDa (± 60 kDa). The T2 fragment has a molecular mass of 28 560 Da but the recombinant form used in this experiment

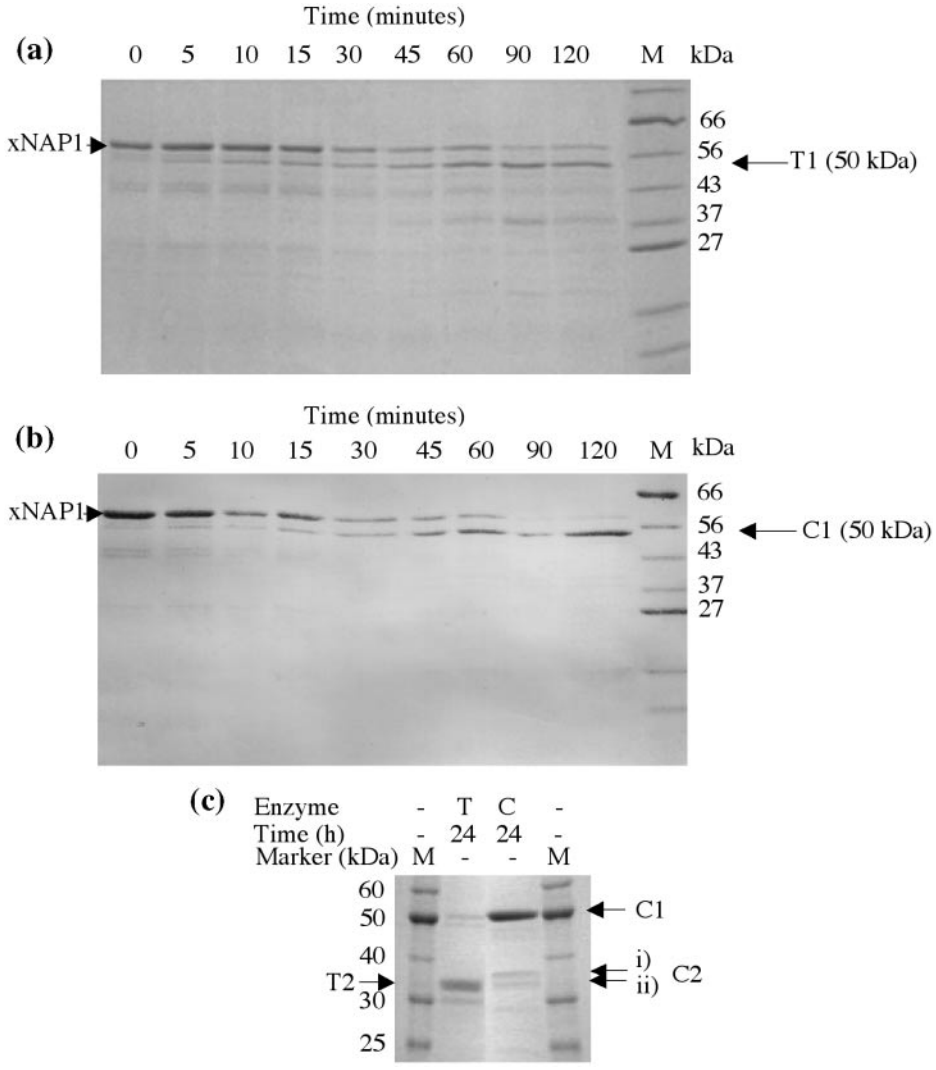

Figure 1. Limited proteolysis of xNAP1 with trypsin and α-chymotrypsin xNAP1 (0.4 mg ml^{-1}) was digested with either trypsin (**a**) or α-chymotrypsin (**b**) at a w/w ratio of 1:10 000 enzyme to substrate. The reaction was incubated at 25°C and stopped with 1 mM PMSF and assayed by SDS–PAGE. The most distinct fragment visible after a 2 h digestion by trypsin is ~50 kDa (T1). A 50 kDa fragment is also visible after 2 h digestion with α-chymotrypsin (C1). (**c**) Further digestion for a period of 24 h with trypsin and with α-chymotrypsin reveals a fragment of ~35 kDa in the trypsin lane (T2). A 24 h digestion with α-chymotrypsin still shows a strong fragment corresponding to C1. Two smaller fragments ~35–37 kDa in size are labelled C2 (i) and (ii).

also includes a 2470 Da his-tag sequence, giving a total molecular weight of 31 030 Da. Thus AUC suggests that the T2 domain forms oligomeric complexes of 12–16 subunits, indicating a predominance of hexadecamers. The data could also be fitted to an octamer–hexadecamer equilibrium model, and K_d values in the range 0.3–2.0 μM gave models that described the data equally well.

Expression of full-length xNAP1, C1 or T2 domains in *Xenopus laevis* embryos leads to identical phenotypic defects

NAP1 has a role in chromatin fluidity that could affect transcription and hence embryonic development. Several studies have shown that NAP1 has an important role in development. Inactivation of NAP1 in *Drosophila* is embryonic lethal (21) and in Xenopus, has also been shown to have a role in tissue specific gene regulation (9,10). xNAP1 has a number of conserved regions, which may be important in these functions, but several of these are missing in the structural domain T2. In particular, the T2 domain lacks the C-terminal acidic regions and hence the PEST sequence. We, therefore, tested how these truncations affected the *in vivo* activity of xNAP1.

To test the *in vivo* activity of the structural domains C1 and T2 we used gain of function analysis by expressing these domains in *Xenopus* embryos. Injection of *in vitro* transcribed mRNA encoding the protein of interest into *Xenopus* is a well-established developmental investigative tool, since over-expression of the target protein can lead to clues to its function *in vivo*. We subcloned the DNA encoding the T2 fragment into the pBUT-2 plasmid, which provides the 5′-UTR (5′-untranslated region) and 3′-UTRs of the globin gene that both stabilizes the mRNA post-injection and maximizes its translation, therefore increasing the levels of encoded protein. We also subcloned two extra constructs (Figure 5a), one based on the proteolytic fragment T2 but

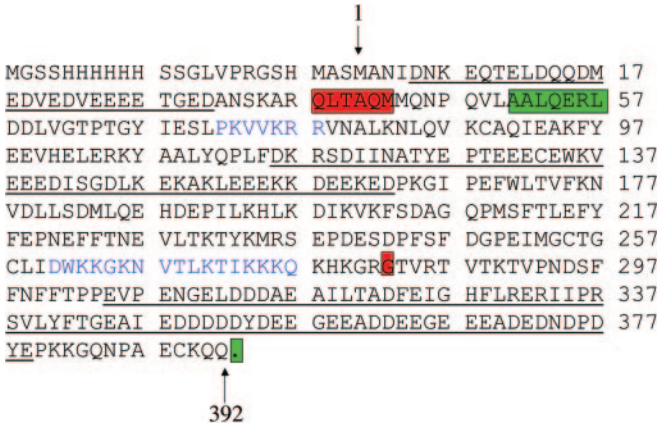

Figure 2. xNAP1 amino acid sequence showing T2 and C1 N-terminal sequences. The N-terminus of the trypsin fragment T2 (red box) and the N-terminus of chymotrypsin fragments C1 (green box) are 13 amino acids apart. The predicted C-terminus of T2 and C1 are also shown (red and green, respectively). Acidic regions are underlined and the bipartite nuclear localization signal is shown in blue. Preceding the wild-type start methionine (numbered 1) is the His-tag sequence present in the recombinant T2 protein.

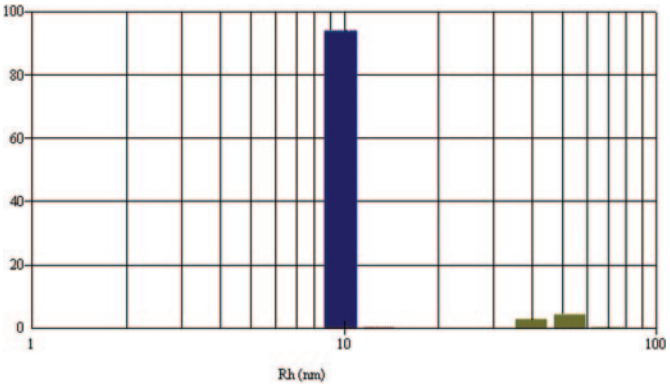

Figure 3. Dynamic light scattering of the T2 domain T2 was purified by metal chelate affinity and size exclusion chromatography. Buffers contained 10% glycerol. The T2 protein sample (0.15 mg ml^{-1}) has one major component, comprising 93.6% (w/w) of the protein with a hydrodynamic radius of 9.6 nm.

without the N-terminal half of the bi-partite NLS and another based on the full-length xNAP1 lacking only the PEST sequence. These proteins were exogenously expressed in *Xenopus* embryos and assayed for any phenotypic changes thereby induced.

The mRNA coding for either xNAP1 or its domains was injected into 1-cell embryos, and these were cultured until stage 36 when phenotypes were observed. Similar phenotypes were observed in stage 36 embryos regardless of whether xNAP1 or truncated xNAP1 mRNA was injected. The affected embryos showed shortening of the embryo along the anterior/posterior axis, microcephaly and reduced mobility (Figure 5b). The proportion of embryos that displayed these effects with 100 pg of injected mRNA varied between 27 and 55% depending on the expressed protein (Table 1). Western blotting showed equal levels of expression of the proteins (data not shown). Uninjected and β-gal mRNA injected control embryos were unaffected.

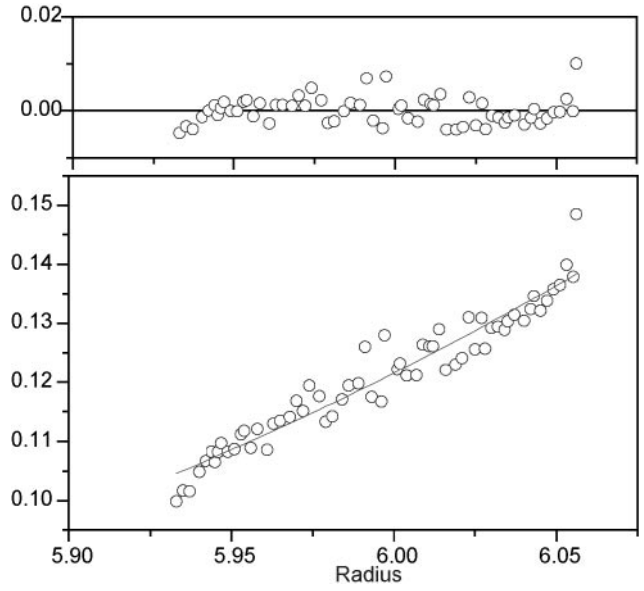

Figure 4. Sedimentation equilibrium of the T2 domain. The sedimentation equilibrium profile of T2 (at 0.14 mg ml^{-1}) in 10% glycerol is shown. The experiment was performed using an Optima™ XLA at 3000 r.p.m., 20°C and the scans taken at 280 nm every 5 h over 24 h. The fitted curve is for a single-species model with $M_r = 430$ kDa.

In previous experiments, we have shown that antisense morpholino-injected NAP knockout embryos are also partially paralysed (10) and, at high morpholino concentrations, have truncated axes (A. Abu-daya and M. J. Guille, unpublished data), correlating with the phenotypes observed here. The fact that gene knockout and over-expression experiments lead to similar phenotypes suggests a 'squelching' mechanism, as discussed below.

DISCUSSION

Here, we report the identification of a structural domain of xNAP1 that retains a functional activity. Digestion of full-length xNAP1 with trypsin or α-chymotrypsin gives rise to two fragments (T1 and C1 respectively). Increased enzyme concentration or longer digestion times with trypsin generated a smaller fragment with an apparent molecular weight of 35 kDa (T2) as assayed by SDS–PAGE, whereas the fragment arising from α-chymotrypsin digestion is largely unaltered by longer digestion times. Therefore, the T2 fragment is likely to represent the smallest stable proteolytic domain of xNAP1, and it is located almost entirely within the larger C1 fragment.

N-terminal sequencing of T2 and C1 successfully defined the N-termini of both the T2 (QLTAQM) and C1 (AALQER) fragments. The N-termini of these two fragments are separated by only 13 amino acids. The T2 N-terminus is nearer to the predicted wild-type start methionine, with no available trypsin site between the T2 and C1 N-termini. However, overall the T2 fragment was the smaller of the two regions, lacking the C-terminal acidic region whereas the C1 fragment extends to the end of the xNAP1 sequence. The truncation of the C-terminus in the T2 fragment leads to the loss of the

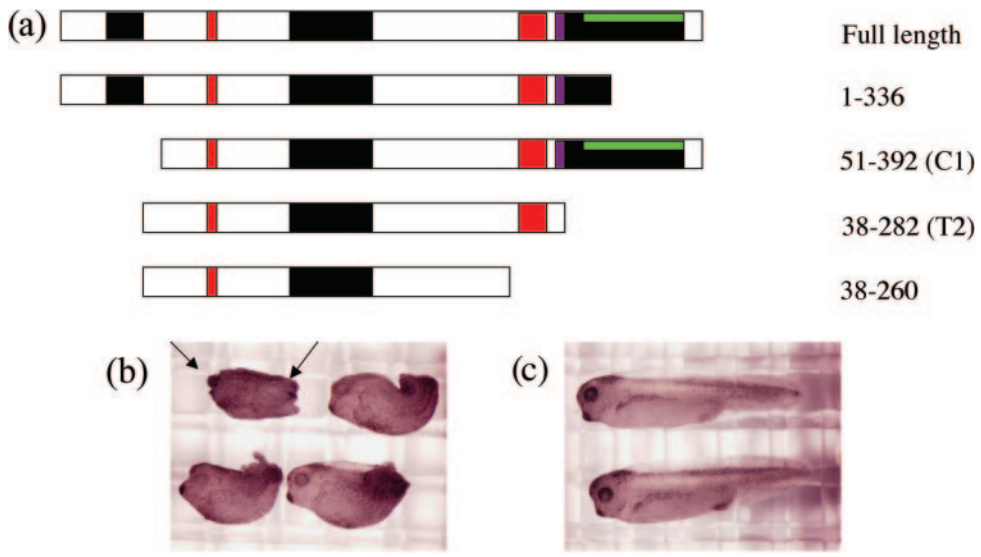

Figure 5. Injection of any of the xNAP1 constructs leads to axial defects. (**a**) Injected constructs are shown with conserved regions indicated. Basic regions marked by a black box, the PEST sequence is shown in green embedded in the C-terminal basic region. The NLS is marked in red and the SFFNFF shown in purple. (**b**) One-cell embryos were injected with 100 pg of either full-length or truncated versions of xNAP1. Un-injected embryos from the same fertilization were cultured in parallel as controls. Embryos were grown in modified bath serum at 18°C until stage 36, fixed in MEMFA (0.5 M MOPS, pH 7.4, 0.5 M EGTA, 0.5 M $MgSO_4$ and 37% formaldehyde) and stored at −20°C in methanol before photographing. All forms of injected xNAP1 gave rise to a shorter A/P axis (lack of head and tail are arrowed) than the un-injected control embryos shown in (**c**).

Table 1. Percentage of embryos effected after injection of 400 pg mRNA from various xNAP1 constructs

Construct	1–392 (full-length)	1–336	51–392 (C1)	38–282 (T2)	38–260
Number of embryos injected	180	180	180	140	140
Percent embryos effected	55	53	30	28	27

SFFNFF and the PEST sequences, both of which have been proposed to have functional roles. Both T2 and C1 fragments contain the NES and the full bi-partite NLS of the complete protein, as well as the conserved KGIPEFWLT sequence.

Full-length NAP1 monomers readily multimerize into complexes varying in size from dimers to octamers and hexadecamers, in a concentration-dependent manner (16). The trypsin fragment T2 retains the ability to multimerize as assayed by dynamic light scattering and sedimentation equilibrium, forming predominantly hexadecameric complexes. It has been proposed that the NAP1 octamers form annular discs, with two discs stacking face to face to form hexadecamers (16). If the negatively charged acidic regions in the wild-type protein were near the octamer–octamer interface, their absence in the T2 domain could favour the hexadecamer by reducing charge repulsion between octamers.

Since these experiments were completed, the first crystal structure of NAP1 (from yeast) has become available (22). The protein crystallizes as a dimer, the dimer interface being maintained by two α-helices in the N-terminal domain of the protein. The remainder of the protein is formed from a core of two further helices (α3 and α4) and six β strands, plus a C-terminal domain consisting of three helices (α6–α8). If the structure of yeast and *Xenopus* NAP1s are similar, as seems likely from their conserved sequences, then we can locate the proteolytic sites for xNAP1 with reference to the structure of yNAP1 when the sequences are aligned.

The N-terminus of the chymotryptic (C1) fragment, Ala51 in xNAP1, corresponds to the start of the first α helix (Q38 in yNAP1), and thus to the first structural domain. The N-terminus of the T2 tryptic fragment (Gln38) is 13 amino acid residues away from this in the unstructured region, but is the nearest basic amino acid to the C1 site. The C-terminus of the T2 fragment (Gly282) corresponds to Lys298 in yNAP1, and lies within the loop between β5 and β6, which is disordered in the crystal structure and hence readily susceptible to proteolysis. Thus, it is clear that the T2 domain of xNAP1 is lacking β6 plus the three C-terminal helices, α6, α7 and α8. Our data suggest that these structural elements are not required for the formation of octamers and hexadecamers.

Considerable evidence now suggests that NAP1 proteins have a role in developmental regulation by controlling transcriptional activity, most likely at the level of chromatin assembly (10,23). We tested the ability of the putative domains C1 (51–392) and T2 (38–282) to affect development relative to the full-length xNAP1 by exogenous expression of these constructs. In addition to the full-length xNAP1 and the putative domains mapped by partial proteolysis, two other constructs were created for expression in *Xenopus* embryos. These consisted of the T2 fragment minus the C-terminal half of the bi-partite NLS (38–260), and a construct lacking much of the C-terminus up to and including the PEST sequence (1–336).

Over-expression of all these constructs led to very similar axial patterning defects that are consistent with interference of NAP function. A 'squelching' model could provide a possible explanation of our observations. In this model, over-expression of exogenous NAP1 protein leads to a

concentration-dependent shift in equilibrium towards formation of hexadecameric NAP1 complexes that have previously been shown to be unable to bind histones (16). We have shown that the T2 domain retains the ability to multimerize *in vitro*. Indeed, the predominance of the hexadecameric form of truncated NAP1 suggests that this complex may be favoured by removal of the acidic tails. Presumably, truncated NAP1 can form mixed hexadecameric complexes with wild-type NAP1, thus transferring endogenous NAP1 into inactive complexes.

Our *in vitro* studies show that the ability to multimerize resides in the central region of the full-length NAP1 protein, and removal of the acidic N- and C-terminal regions may indeed favour formation of larger multimers. *In vivo* injection of a range of truncated xNAP1 constructs into *Xenopus* embryos leads to axial defects. The ability to produce this phenotype resides primarily in the central 51–260 amino acid sequence and may reflect the ability of this region to multimerize into a non-histone binding hexadecamer.

ACKNOWLEDGEMENTS

The authors thank Dr James Taylor and Dr Anastasia Callaghan for advice and assistance with the analysis of AUC data. The authors are grateful to BBSRC for a project grant and University of Portsmouth (IBBS) for a graduate student bursary. Funding to pay the Open Access publication charges for this article was provided by the University of Portsmouth.

Conflict of interest statement. None declared.

REFERENCES

1. Ishimi,Y. and Kikuchi,A. (1991) Identification and molecular cloning of yeast homolog of nucleosome assembly protein I which facilitates nucleosome assembly *in vitro*. *J. Biol. Chem.*, **266**, 7025–7029.
2. Earnshaw,W.C., Honda,B.M., Laskey,R.A. and Thomas,J.O. (1980) Assembly of nucleosomes: the reaction involving *X.laevis* nucleoplasmin. *Cell*, **21**, 373–383.
3. Kleinschmidt,J.A. and Seiter,A. (1988) Identification of domains involved in nuclear uptake and histone binding of protein N1 of *Xenopus laevis*. *EMBO J.*, **7**, 1605–1614.
4. Ito,T., Bulger,M., Kobayashi,R. and Kadonaga,J.T. (1996) *Drosophila* NAP-1 is a core histone chaperone that functions in ATP-facilitated assembly of regularly spaced nucleosomal arrays. *Mol. Cell. Biol.*, **16**, 3112–3124.
5. Park,Y.J., Chodaparambil,J.V., Bao,Y., McBryant,S.J. and Luger,K. (2005) Nucleosome assembly protein 1 exchanges histone H2A-H2B dimers and assists nucleosome sliding. *J. Biol. Chem.*, **280**, 1817–1825.
6. Chakravarthy,S., Park,Y.J., Chodaparambil,J., Edayathumangalam,R.S. and Luger,K. (2005) Structure and dynamic properties of nucleosome core particles. *FEBS Lett.*, **579**, 895–898.
7. Shikama,N., Chan,H.M., Krstic-Demonacos,M., Smith,L., Lee,C.W., Cairns,W. and La Thangue,N.B. (2000) Functional interaction between nucleosome assembly proteins and p300/CREB-binding protein family coactivators. *Mol. Cell. Biol.*, **20**, 8933–8943.
8. Ito,T., Ikehara,T., Nakagawa,T., Kraus,W.L. and Muramatsu,M. (2000) p300-mediated acetylation facilitates the transfer of histone H2A-H2B dimers from nucleosomes to a histone chaperone. *Genes Dev.*, **14**, 1899–1907.
9. Steer,W.M., Abu-Daya,A., Brickwood,S.J., Mumford,K.L., Jordanaires,N., Mitchell,J., Robinson,C., Thorne,A.W. and Guille,M.J. (2003) *Xenopus* nucleosome assembly protein becomes tissue-restricted during development and can alter the expression of specific genes. *Mech. Dev.*, **120**, 1045–1057.
10. Abu-Daya,A., Steer,W.M., Trollope,A.F., Friedeberg,C.E., Patient,R.K., Thorne,A.W. and Guille,M.J. (2005) Zygotic nucleosome assembly protein-like 1 has a specific, non-cell autonomous role in hematopoiesis. *Blood*, **106**, 514–520.
11. Fujii-Nakata,T., Ishimi,Y., Okuda,A. and Kikuchi,A. (1992) Functional analysis of nucleosome assembly protein, NAP-1. *J. Biol. Chem.*, **267**, 20980–20986.
12. Li,M., Strand,D., Krehan,A., Pyerin,W., Heid,H., Neumann,B. and Mechler,B.M. (1999) Casain kinase 2 binds and phosphorylates the nucleosome assembly protein-1 (NAP1) in *Drosophila melanogaster*. *J. Mol. Biol.*, **293**, 1067–1084.
13. Miyaji-Yamaguchi,M., Kato,K., Nakano,R., Akashi,T., Kikuchi,A. and Nagata,K. (2003) Involvement of nucleocytoplasmic shuttling of yeast Nap1 in mitotic progression. *Mol. Cell. Biol.*, **23**, 6672–6684.
14. McBryant,S.J., Park,Y.J., Abernathy,S.M., Laybourn,P.J., Nyborg,J.K. and Luger,K. (2003) Preferential binding of the histone $(H3\text{-}H4)_2$ tetramer by NAP1 is mediated by the amino-terminal histone tails. *J. Biol. Chem.*, **278**, 44574–44583.
15. McBryant,S.J. and Peersen,O.B. (2004) Self-association of the yeast nucleosome assembly protein 1. *Biochemistry*, **43**, 10592–10599.
16. Toth,K.F., Mazurkiewicz,J. and Rippe,K. (2005) Association states of nucleosome assembly protein 1 and its complexes with histones. *J. Biol. Chem.*, **280**, 15690–15699.
17. Smith,J.C. and Slack,J.M.W. (1983) Dorsalisation and neural induction: properties of the organiser in *Xenopus laevis*. *J. Embryol. Exp. Morphol.*, **78**, 299–317.
18. Nieuwkoop,P.D. and Faber,J. (1967) *Normal Table of Xenopus laevis*. Daudin, North Holland, Amsterdam.
19. Moore,W.M. and Guille,M.J. (1999) Preparation and testing of synthetic mRNA for microinjection. In Guille,M.J. (ed.), *Molecular Methods in Developmental Biology*. Humana Press, NJ, Vol. 127, pp. 99–110.
20. Guille,M. (1999) Microinjection into Xenopus Oocytes and Embryos. In Guille,M. (ed.), *Molecular Methods in Developmental Biology*. Humana Press, NJ, Vol. 127, pp. 111–125.
21. Lankenau,S., Barnickel,T., Marhold,J., Lyko,F., Mechler,B.M. and Lasnkenau,D.H. (2003) Knockout targeting of the *Drosophila* NAP1 gene and examination of DNA repair tracts in the recombination products. *Genetics*, **163**, 611–623.
22. Park,Y.-J. and Luger,K. (2006) The structure of nucleosome assembly protein 1. *Proc. Natl Acad. Sci. USA*, **103**, 1248–1253.
23. Rodriguez,P., Munroe,D., Prawitt,D., Chu,L.L., Bric,E., Kim,J., Reid,L.H., Davies,C., Nakagama,H., Loebbert,R. *et al.* (1997) Functional characterisation of a human nucleosome assembly protein-2 (NAP1L4) suggests a role as a histone chaperone. *Genomics*, **44**, 253–265.